Journal of Medicinal Chemistry

Article

Discovery, Optimization, and Characterization of Novel Chlorcyclizine Derivatives for the Treatment of Hepatitis C Virus Infection

Shanshan He, Jingbo Xiao, Andrés E Dulcey, Billy Lin, Adam Rolt, Zongyi Hu, Xin Hu, Amy Q Wang, Xin Xu, Noel Southall, Marc Ferrer, Wei Zheng, T Jake Liang, and Juan J Marugan

J. Med. Chem., **Just Accepted Manuscript** • DOI: 10.1021/acs.jmedchem.5b00752 • Publication Date (Web): 24 Nov 2015

ACS Publications

Journal of Medicinal Chemistry is published by the American Chemical Society. 1155 Sixteenth Street N.W., Washington, DC 20036

Discovery, Optimization, and Characterization of Novel Chlorcyclizine Derivatives for the Treatment of Hepatitis C Virus Infection

Shanshan He,[§,†] Jingbo Xiao,[§,‡] Andrés E Dulcey,[‡] Billy Lin,[†] Adam Rolt,[‡] Zongyi Hu,[†] Xin Hu,[‡] Amy Q. Wang,[‡] Xin Xu,[‡] Noel Southall,[‡] Marc Ferrer,[‡] Wei Zheng,[‡] T. Jake Liang,[†] and Juan J. Marugan*[‡]*

[†]Liver Diseases Branch, National Institute of Diabetes and Digestive and Kidney Diseases, National Institutes of Health, 10 Center Drive, Bethesda, Maryland 20892

[‡]Division of Pre-Clinical Innovations, National Center for Advancing Translational Sciences, National Institutes of Health, 9800 Medical Center Drive, Rockville, Maryland 20850

KEYWORDS

hepatitis C virus, antihistamines, chlorcyclizine, antivirals

ABSTRACT

Recently we reported that chlorcyclizine (CCZ, **Rac-2**), an over-the-counter antihistamine piperazine drug, possesses *in vitro* and *in vivo* activity against hepatitis C virus. Here, we describe structure-activity relationship (SAR) efforts that resulted in the optimization of novel chlorcyclizine derivatives as anti-HCV agents. Several compounds exhibited EC_{50} values below 10 nM against HCV infection, cytotoxicity selectivity indices above 2000, and showed improved *in vivo* pharmacokinetic properties. The optimized molecules can serve as lead preclinical candidates for the treatment of hepatitis C virus infection and as probes to study hepatitis C virus pathogenesis, and host-virus interaction.

INTRODUCTION

Hepatitis C virus (HCV) is an enveloped positive-stranded RNA virus of the *Flaviviridae* family. The HCV replication cycle is initiated by virions entering the host cell via interaction with cell surface receptors. Following pH-dependent fusion and uncoating, the HCV RNA genome is translated. The resulting polyprotein undergoes proteolytic cleavage into structural (core, E1, and E2) and nonstructural (p7, NS2, NS3, NS4A, NS4B, NS5A, and NS5B) proteins. After RNA replication, HCV undergoes assembly, maturation and secretion processes.[1, 2]

HCV leads to acute and chronic inflammatory hepatic infections that often progress toward chronic liver diseases, including cirrhosis, with an elevated risk of developing hepatocellular carcinoma. There is no vaccine for HCV to date.[3] Besides there being around 180 million people chronically infected worldwide with HCV, the standard of care for many years has been limited to interferon α (IFN-α) in combination with ribavirin (RBV).[4, 5] This combination therapy is partially effective with serious adverse effects. Drug discovery efforts during the past 20 years

led to a new paradigm for HCV treatment, which is marked by the recent approval of multiple direct-acting antivirals (DAAs) for interferon-free regimens.[2, 6, 7] The DAAs inhibit certain replication steps in the HCV replication cycle by directly targeting viral proteins, such as NS3/4A proteases, NS5A or NS5B polymerase.[8] Viral rebounds were often observed during monotherapy of these DAAs due to selection of drug-resistant viral mutants. Thus, the clinical application of DAAs is mostly limited to combination regimens, which face challenges including additional side effects, complex administration and drug-drug interactions.[2] Sofosbuvir,[9] a DAA that has been approved for interferon-free regimen, costs more than $80,000 during a typical 12-week course of treatment alone, raising concerns about the affordability of DAAs in order to globally impact the burden of HCV disease.[10, 11] Host-targeting agents (HTAs), on the other hand, inhibit host factors that are essential in the viral replication cycle. Promising host-factor targets of HTAs include entry factors, components of viral replication complex cyclophilin A, and miR122 that binds to viral RNA to facilitate replication.[1] There is a higher genetic barrier to develop resistance to HTAs.[12] Moreover, HTAs can also be used as chemical probes to elucidate anti-HCV mechanisms and host-virus interactions. However, few HTAs candidates are in the anti-HCV drug discovery pipeline, possibly due to the nature of primary drug screen assays that were mostly based on certain viral proteins or HCV replicons. Overall, there is still need to improve the current therapeutic regimens by exploring novel anti-HCV targets and small molecules.

Recently, we reported the anti-HCV activity of chlorcyclizine (CCZ, **Rac-2**), discovered through the screening of the NCGC Pharmaceutical Collection (NPC), in a cell-based anti-HCV quantitative high-throughput screening (qHTS) platform.[13-15] The hit compound chlorcylizine HCl (CCZ (**Rac-2**), Figure 1) showed potent *in vitro* anti-HCV activity and preferable liver

distribution in mouse models, as well as *in vivo* efficacy against HCV infection in Alb-uPA/SCID chimeric mouse model engrafted with primary human hepatocytes.[14] CCZ (**Rac-2**) was also reported by Chamoun-Emanuelli et al. to block HCV entry, possibly via a cholesterol-dependent pathway.[16] However the target and precise mechanism of action of CCZ (**Rac-2**) in inhibiting HCV entry remains unknown. Here, we present an SAR study aiming to optimize CCZ (**Rac-2**) for an anti-HCV application focusing on the following features: generation of a non-chiral lead, improvement of its anti-HCV potency, modulation of its physicochemical properties to potentially reduce CNS exposure, reduction or elimination of its antihistamine activity, and improvement of pharmacokinetic properties. The resulting lead compounds in this series, represented by non-chiral compound **30**, exhibited increased anti-HCV activity and selectivity (up to 19-fold and 8-fold, respectively) and improved *in vivo* pharmacokinetics properties. The optimized lead compounds merit further preclinical development for the treatment of hepatitis C.

RESULTS

The synthesis of CCZ analogs is displayed in Schemes 1-5. Scheme 1A shows the synthesis of asymmetrical CCZ derivatives. Thus, following modified literature procedrues, the corresponding aldehyde or ketone underwent reductive amination with commercially available chiral **(R)-1** or **(S)-1**, and $NaBH_3CN$ in the presence of acetic acid (compounds **10-15**)[28] or *p*-toluenesulfonic acid (compound **(S)-18**) using an alcoholic solvent, to afford the corresponding *N*-alkylated derivatives. $Ti(OiPr)_4$ was required to carry out the reductive amination of the cyclopentyl (**(S)-16**) and cyclohexyl (**(S)-17**) derivatives.[17] Acylation of **(S)-1** with acetyl chloride afforded *N*-acyl derivative **(S)-19**. Deuterated derivatives **(R)-20** and **(S)-20** where synthesized from **(R)-1** and **(S)-1** with CD_3I in the presence of aqueous NaOH. Likewise,

trifluorinated derivatives **(R)-21** and **(S)-21** were prepared from the common chiral starting material and trifluoroethyl triflate in the presence of K_2CO_3.

Scheme 1B displays the synthesis of racemic CCZ analogs with a solubilizing polyethylene glycol side chain. Starting from the commercially available hydroxyzine (**Rac-5**), introduction of the phthalimido moiety via standard Mitsunobu conditions afforded **Rac-22**. Subsequent hydrazine mediated deprotection afforded primary amine **Rac-23**. Elongation of the solubilizing side chain was obtained by alkylating **Rac-5** to produce *N*-Boc derivative **Rac-24**, which was deprotected to the free amine **Rac-25** and subsequently acylated to afford **Rac-26** (Scheme 1B).

The synthesis of achiral dichlorcyclizine derivatives is displayed in scheme 2A. Starting from dichlorobenzophenone **27**, $NaBH_4$ mediated reduction of the ketone, followed by chlorination with $SOCl_2$ afforded chloride **28**, which was used to alkylate a variety of cyclic amine derivatives following modified literature procedures to yield compounds **29-33** (Scheme 2A).[29-31] Piperazine derivative **29** was further alkylated, following a modified literature procedure, to produce the diehtylene glycol-containing compound **34**,[32] which was further elongated to the pentaethylene glycol amine **35**. To probe the halogen effect on the cyclizine scaffold, compounds **38** and **39** were prepared according to Scheme 2B, via reductive amination of acetaldehyde with the corresponding piperazines **36** and **37** in the presence of $NaBH_3CN$ and acetic acid in methanol.

Cyclizine scaffold modification via exchange of the central tertiary carbon with the nitrogen analog is displayed in Scheme 3A, where methyl piperidone underwent reductive amination with the corresponding aniline **40** and **41** to afford the intermediate amines **42** and **43**, which subsequently underwent *N*-arylation under Buchwald conditions to afford amines **44** and **45**. The last modification studied was the introduction of rigidity into the cyclizine scaffold. As displayed

in Scheme 3B, this was accomplished by starting from the commercial bromofluorenone **46**, which was reduced to the alcohol with $NaBH_4$, and subsequently converted to the chloride **47** with $CaCl_2$ and concentrated HCl. Chloride **47** was used to alkylate *N*-ethyl piperazine to afford the cyclizine rigid analog **48** (Scheme 3B).

Tables 1-3 disclose the activity of synthesized compounds in our structural/chemical modification study centered around CCZ (**Rac-2**). The anti-HCV activity was reported in EC_{50} values (concentration of compound inhibiting 50% of viral levels in comparison with DMSO control) using the HCV-Luc (HCV JFH-1 strain (GT2a) with insertion of the luciferase reporter gene) infection assay. The cytotoxicity was measured by CC_{50} values (concentration of compound exhibiting 50% cytotoxicity in comparison with DMSO control) evaluated with an ATPlite assay in Huh7.5.1 cells, the same cell line used for measuring the antiviral activity. Thus, the activities of the hit compound, racemic CCZ (**Rac-2**) and its enantiomers (**(R)-2** and **(S)-2**) were confirmed as having good selectivities (selective indices = 1132~1875, Table 1). Nor-CCZ (compound **1**), a known *in vivo* metabolite of CCZ, showed comparable anti-HCV activity, but with reduced selectivity (Table 1). It should be noted with interest nor-CCZ's lack of antihistamine activity (Table 4).[18-20]

In Table 1, we addressed the effect of two types of structural modifications: (1) chiral configurations, and (2) side chains off the piperazine ring. The enantiomers of compounds **1**, **2**, **10**, **11**, **12**, **13**, **15**, **20**, and **21** showed comparable EC_{50} and CC_{50} values, suggesting that the chiral configuration of CCZ analogs does not have a major effect on the antiviral activity and selectivity. With compounds **10**, **11**, **12**, **13**, and **18**, we investigated the effect of the length of the aliphatic chain on the anti-HCV activity. When the number of carbons was less than 4, analogs showed comparable activity in the range of low double-digit nanomolar and comparable

selectivity to CCZ (**Rac-2**), regardless of whether the chain was linear or branched. Chains with a carbon number of 4 led to decreased activity as shown for compounds **12** and **13**. Surprisingly, compound **16**, having a cyclopentyl ring exhibited an improved activity (EC_{50} = 19 nM) while compound **17,** having a cyclohexyl ring, showed an activity in the expected range (EC_{50} = 177 nM), comparable to compounds **12** and **13**. Additionally, acetylation of the piperazine ring dramatically reduced the potency of analogue **19** to double-digit micromolar value. Introduction of a bulky substituted benzyl group also reduced the anti-HCV activity (compound **14**, EC_{50} = 456 nM). Deuterium, introduced in the side chain of compounds **20** and **15** with the aim of increasing their metabolic $t_{1/2}$, did not impact their anti-HCV activity, and indeed lead to a slightly improved $t_{1/2}$ value (2.9 h for **(R)-15** in comparison with 2.2 h for **(R)-10** in rat microsomal stability assay). Moreover, the trifluoromethyl group in compound **21** led to a complete loss of activity, potentially indicating that the pKa value of the tertiary amine was important for the anti-HCV activity.

The side effects of CCZ (**Rac-2**) include drowsiness, dizziness and headache, attributed to its ability to cross the blood-brain barrier and its CNS penetration. For this reason, first generation antihistamine drugs were replaced by analogs like cetirizine, with reduced CNS-related side effects.[21] In order to explore the possibility of reducing the CNS penetration of our molecules, we further expanded our synthetic efforts introducing oligoethylene glycol side chains. This structural modification would increase the molecular weight, solubility, total polar surface area and number of free rotatable bonds, also potentially leading toward longer pharmacokinetic half-lives. By using ethylene glycol or polyethylene glycol as linker, we explore the effect of introducing a series of functional groups at the terminal position. Compound **Rac-3** having a terminal carboxylic acid, completely lost the anti-HCV activity, potentially due to lack of cell

permeability. Moderate activities in the range of triple-digit nanomolar to single-digit micromolar were observed with carboxamide-substituted compounds **Rac-4**, **Rac-22**, **Rac-24**, and **Rac-26** (Table 1). Compounds **Rac-5**, **Rac-23** and **Rac-25,** having hydroxyl or amino groups at the chain terminal position, displayed high anti-HCV activity and moderate cytotoxicity. It was noteworthy that a 6-fold increased activity and retained selectivity was observed with compound **Rac-23** (EC_{50} values below 8 nM with selective indices above 1000) (Table 1).

Table 2 shows the activity of analogs exploring different phenyl ring substituents. Thus, elimination of the para-chloro substituent reduced the activity from double-digit nanomolar (compound **Rac-2**, EC_{50}= 44 nM) to single-digit micromolar (compound **6**, EC_{50}= 1.14 μM). Introduction of an additional para-cloro substituent in the other ring slightly increased the activity (compound **30**, EC_{50}= 17 nM). Following similar trend, non-chiral dichloro compounds **29**, **31**, **34** and **35** also showed increased activity (1.3 ~ 8.7-fold) in comparison with the corresponding monochloro analogues **Rac-1**, **(S)-10**, **Rac-5**, and **Rac-25**. In general, the introduction of Br substituents led to comparable activity and selectivity to the corresponding Cl substituted compounds as shown in **Rac-36**, **Rac-37**, **Rac-38**, and **Rac-39**.

Structural modifications to the piperazine core are displayed in Table 3, where compounds **Rac-2**, **29**, **6** and **Rac-38** were included for comparison. Compound **Rac-7**, having a one carbon extension of the piperazine ring, retained the activity but led to increased cytotoxicity. The replacement of the piperazine ring with other ring structures in compounds **32**, **33**, and **9** led to a dramatic loss of activity. In contrast, compounds **44**, **45**, and **8** retained the anti-HCV activity and selectivity.

Compound **48**, which has a rigid cyclizine scaffold, showed an EC_{50} value that was more than 1 μM, indicating that the conformation of the rings was important for the anti-HCV activity.

From our SAR studies, we selected a number of lead compounds based on their anti-HCV activity, selectivity and structure diversity for an expanded characterization (Table 4). The cytotoxicity of these molecules was further evaluated in HepG2 cells and primary human hepatocytes. All compounds showed less than 1.8-fold difference in CC_{50} values in these two cell types in comparison with Huh7.5.1 cells (used for our anti-HCV activity assay), with the exception of compound **31,** which was less cytotoxic in HepG2 cells than in Huh7.5.1 (approximately 3-fold higher CC_{50}) (Table 4). The H1HR antagonistic activity of the chosen compounds were evaluated by measuring their capacity to block the beta-arrestin internalization signal induced by Histamine. The numeric value observed corresponds to the percentage of activation induced by Histamine (250 nM) in the presence of 10 nM of compound, using CCZ (**Rac-2**) and **(S)-1** as the positive and negative controls respectively. Shown in Table 4, the results of CCZ (**Rac-2**) and **(S)-1** were consistent with previously reported results.[14] Lead compounds with R_3 = H (compounds **(S)-1** and **29**) showed very low H1HR inhibition (approximately 10%). Meanwhile when R_3 = Me, Et or medium oligoethylene glycol chain, the H1HR inhibitory effects were generally lower than that of CCZ (**Rac-2**) (compounds **Rac-23, 30, 31,** and **34**), and **(S)-10** showed approximately 4-fold lower inhibition. Compound **Rac-25** having a long oligoethylene glycol chain, showed more than 3-fold lower inhibitory effect towards H1HR.

Additionally, HCV replication cycle assays were carried out to study the target stage of the CCZ analogues in the HCV replication cycle. The lead compounds exhibited potent inhibition in the HCV single-cycle assay, in which single-round infectious HCV (HCVsc) can infect

hepatocytes but does not assemble into new virions (Table 4).[13, 14] The activity suggested that the CCZ analogues inhibited early steps of the HCV replication cycle prior to assembly. The analogues were tested in the HCV pseudoparticle (HCVpp) assay and the HCV subgenomic replicon assay,[13] which detect whether the compounds target HCVpp entry and HCV replication, respectively. The HCVpp assay applies defective retroviral particles that harbor the HCV envelope glycoproteins to assess viral entry inhibition.[13, 22-24] No significant inhibitory effect was observed in the HCVpp (genotype 1a and 1b) assay with the lead compounds, except for **Rac-23** possibly due to cytotoxicity (Table 4). To address viral specificity in the entry process, vesicular stomatitis virus G pseudoparticle (VSV-Gpp) and murine leukemia virus pseudoparticle (MLVpp) were tested as control, in which no inhibitory effect was detected (Table 4). It is worth noting that the lack of HCVpp inhibition of a compound does not necessarily exclude virus entry as a mode of action. A compound could be targeting an entry step that is not otherwise captured by the HCVpp system. Multiple HCV entry inhibitors were reported without HCVpp inhibitory effect, including NPC1L1 antagonist ezetimibe and human apolipoprotein E peptides.[25, 26] In the genotype 2a HCV replicon cell line, all the lead compounds failed to reduce below 60% the replicon activity, as compared tothe DMSO control, indicating that RNA replication was not the target of these analogues (Table 4).

Moreover**,** besides the *in vitro* physical properties of the chosen lead compounds, their *in vitro* metabolic properties were also evaluated using human, mouse and rat microsomes. Compounds **29**, **30**, and **34** showed preferable human microsomal stability ($t_{1/2} \geq 30$ min), while maintaining reasonable solubility.

In vivo pharmacokinetics and tissue distribution levels of compound **30** was measured in mice after a single dose of 10 mg/kg through intraperitoneal (i.p.) route (Table S1). The half-life in

liver was 8.5 h, which was an improvement in comparison with the half-lives of (S)-CCZ [compound **(S)-2**] and (S)-nor-CCZ [compound **(S)-1**] (1.99 h and 4.7 h, respectively) measured under the same conditions (Figure 2A and C).[14] Preferential liver distribution was also observed, as shown by the liver/plasma AUC_{last} ratio of 16 (Figure 2C). Within 24 h after a single dose of 10 mg/kg, the liver concentration of compound **30** (56.9 ~ 5.29 μM) was dramatically above its *in vitro* EC_{50} values (0.017 μM). To detect any potential hepatotoxicity effect, the alanine transaminase (ALT) levels[27] in the mouse serum were measured (Figure 2B). When treated with compound **30**, the ALT levels were around or below 80 U/L at most time points except when t = 2 and 4 h, which may suggest a potential transient mild liver toxicity. From these observations we concluded that there was not a clear correlation between the ALT levels and liver concentration of the compounds. To study whether the mild elevations of ALT level were due to compounds or vehicle, a control study was carried out dosing vehicle only. The ALT level was elevated at multiple time points with the treatment of vehicle only (Figure 2B). Overall, we concluded that no clear hepatotoxicity was detected with the treatment of compound **30** in this condition.

To evaluate the capacity of these compounds to potentially impact other viruses in the *Flaviviridae* family, their antiviral activity was tested against dengue virus. Both lead compounds **(S)-10** and **30** showed EC_{50} values in DENV-RVPs assay that were approximately 1000-fold more than their EC_{50} values against HCV-Luc infection (Table 4), together with CC_{50} values consistent with observation when cells were infected with HCV-Luc (Table S1). The selective indices were below 5 for both compounds against dengue virus. Furthermore, the activity of **(S)-10** was submitted for evaluation in the NIAID antiviral screen against 13 types of viruses: hepatitis B virus, HCV replicon, herpes simplex virus-1, human cytomegalovirus,

vaccinia virus, dengue virus, influenza A (H1N1) virus, respiratory syncytial virus, SARS coronavirus, poliovirus 3, Rift Valley fever virus, Tacaribe virus, and Venezuelan equine encephalitis virus. Little or no antiviral activity was detected (selective index < 10 and/or $EC_{50} \geq$ 1 μM), suggesting that the antiviral effects and mechanism of these analogues were HCV-specific.

DISCUSSION

Besides the advancement in developing efficacious treatments for chronic HCV infection, the cost and side effects of current approved methods point to the direction of developing alternative approaches to therapeutically intervene in the disease. In this sense, in our previous study, we disclosed the *in vitro* and *in vivo* anti-HCV properties of chlorcyclizine (CCZ, **Rac-2**), a first generation antihistamine compound approved for over-the-counter use.[14] Its affordability and established clinical safety profile make CCZ (**Rac-2**) an attractive candidate for repurposing toward chronic HCV infection (https://clinicaltrials.gov/ct2/show/NCT02118012). Additionally, we decided to carry out structural modifications, *in vitro* and *in vivo* studies to further optimize this series with the aim of improving their anti-HCV profile. We focused the chemical modifications on four major structural motifs: chirality, side chains off the piperazine ring, substituents on the phenyl rings, and modifications on the piperazine core. As summarized in Figure 3, chirality had little effect on the antiviral activity and selectivity. Dual para-chloro substitution on the aromatic rings led to more potent non-chiral analogues. Furthermore, the introduction of oligoethylene glycol off the piperazine ring nitrogen improved the activity without compromising the selectivity. Most of the structure modifications in the piperazine core were not tolerated, suggesting that its geometry and its pKa value were important for the anti-

HCV activity of the series. Selected lead compounds were also analyzed for additional assessment of cytotoxicity in HepG2 hepatocytes and primary human hepatocytes. They showed similar profiles as those observed in Huh7.5.1 cells, suggesting that the cytotoxicity evaluation in Huh7.5.1 cells in parallel with HCV infection assay provides a good estimation of the cytotoxicity in human hepatocytes. Overall, the lead compounds in Table 4 exhibited excellent antiviral activity and selectivity in host cells (SI = 8608 ~ 201). One of the goals of this medicinal chemistry study was to eliminate the antihistamine side effect of CCZ (**Rac-2**), which was achieved with lead compounds having R_3 = H or long ethylene glycol chains (compounds **29** and **Rac-25**).

In the HCV replication cycle assays, the lead compounds showed similar inhibitory patterns as CCZ (**Rac-2**), displaying a dramatic inhibition in early stage HCV infection (in HCVsc assay) but no inhibition on HCVpp entry or in the HCV replicon system. Although the exact mechanism of action of CCZ (**Rac-2**) is still under investigation, the observations here strongly suggest that the lead compounds likely follow the same mechanism of action as CCZ (**Rac-2**), only with improved activity and selectivity.

In vitro microsomal stability assays were carried out to evaluate the potential metabolic stability of the lead compounds. Among compounds **29**, **30**, and **34** with $t_{1/2} > 30$ min in human microsomes, compounds **30** was selected for *in vivo* pharmacokinetic mouse studies because of its lower *in vitro* cytotoxicity. Compound **30** showed improved PK properties in comparison with (S)-CCZ (**(S)-2**), namely a longer half-life, while retaining a high liver/plasma ratio.

CONCLUSION

Besides the progress in the treatment of chronic HCV infection, among other issues, the global affordability is still an important factor to consider within the current treatment options. Repurposing the over-the-count drug CCZ (**Rac-2**) may offer an affordable treatment for chronic HCV infection.[14] Additionally, we presented a chemical/structural modification study, which resulted in optimized, non-chiral well-tolerated CCZ analogues with improved anti-HCV potency and pharmacokinetic properties that are able to provide good coverage in the liver at very reasonable doses. The lead compounds inhibited HCVsc infection without affecting HCVpp entry or HCV replication in the replicon assay, which is similar to the findings for CCZ (**Rac-2**), suggesting an unaltered mechanism of action. The lead compounds showing overall improved properties, will be selected for *in vivo* anti-HCV efficacy studies and potentially for further preclinical drug development efforts with the aim of moving additional compounds of this series toward anti-HCV human clinical trials.

EXPERIMENTAL SECTION

Chemistry. All air or moisture sensitive reactions were performed under positive pressure of nitrogen with oven-dried glassware. Anhydrous solvents such as dichloromethane, *N*,*N*-dimethylformamide (DMF), acetonitrile, methanol and triethylamine were purchased from Sigma-Aldrich (St. Louis, MO). Preparative purification was performed on a Waters semi-preparative HPLC system (Waters Corp., Milford, MA). The column used was a Phenomenex Luna C_{18} (5 micron, 30 x 75 mm; Phenomenex, Inc., Torrance, CA) at a flow rate of 45.0 mL/min. The mobile phase consisted of acetonitrile and water (each containing 0.1% trifluoroacetic acid). A gradient of 10% to 50% acetonitrile over 8 min was used during the purification. Fraction collection was triggered by UV detection at 220 nM. Analytical analysis

was performed on an Agilent LC/MS (Agilent Technologies, Santa Clara, CA). Method 1: A 7-min gradient of 4% to 100% acetonitrile (containing 0.025% trifluoroacetic acid) in water (containing 0.05% trifluoroacetic acid) was used with an 8-min run time at a flow rate of 1.0 mL/min. Method 2: A 3-min gradient of 4% to 100% acetonitrile (containing 0.025% trifluoroacetic acid) in water (containing 0.05% trifluoroacetic acid) was used with a 4.5-min run time at a flow rate of 1.0 mL/min. A Phenomenex Luna C_{18} column (3 micron, 3 x 75 mm) was used at a temperature of 50 °C. Purity determination was performed using an Agilent diode array detector for both Method 1 and Method 2. Mass determination was performed using an Agilent 6130 mass spectrometer with electrospray ionization in the positive mode. ^{1}H NMR spectra were recorded on Varian 400 MHz spectrometers (Agilent Technologies, Santa Clara, CA). Chemical shifts are reported in ppm with undeuterated solvent (DMSO at 2.49 ppm) as internal standard for DMSO-d_6 solutions. All of the analogs tested in the biological assays have a purity of greater than 95% based on both analytical methods.

High resolution mass. spectrometry was recorded on Agilent 6210 Time-of-Flight (TOF) LC/MS system. Confirmation of molecular formula was accomplished using electrospray ionization in the positive mode with the Agilent Masshunter software (Version B.02). Enantiomerically pure compounds were purified to > 99% purity using supercritical fluid chromatography (SFC) preparative systems at Lotus Separations, LLC (Princeton, NJ, USA). Compounds **Rac-1**, **(S)-1**, and **(R)-1** were purchased from Albany Molecular Research (Albany, NY, USA). Compounds **Rac-2**, **(S)-2**, and **(R)-2** were purchased from MP Biomedicals (Santa Ana, CA, USA). Compounds **Rac-3** and **6** were purchased from Prestwick Chemical (France). Compound **Rac-5** was purchased from TimTec (Newark, DE, USA). Compound **Rac-7** was purchased from Biomol (Germany). Compounds **8** and **9** were purchased from Sigma-Aldrich

(St. Louis, MO, USA). Compounds **10**,[28] **12**,[28] **29**,[29] **30**,[30] **32**,[31] **33**,[31] and **34**,[32] were synthesized by modified literature procedures. Compounds **Rac-36** and **Rac-37** were purchased from Vitas-M Laboratory (Netherlands).

(S)-1-((4-Chlorophenyl)(phenyl)methyl)-4-ethylpiperazine ***((S)-10)****.* A solution of **(S)-1** (50.0 mg, 0.174 mmol) in methanol (MeOH) (2.00 mL) was treated at room temperature with acetaldehyde (38.4 mg, 0.872 mmol), $NaBH_3CN$ (32.9 mg, 0.523 mmol) and acetic acid (30.0 mL, 0.523 mmol). The reaction mixture was stirred at room temperature overnight and then quenched with 1 N NaOH solution. The mixture was dried by blowing air, the residue was re-disolved in DMSO, filtered and purified by preparative HPLC to afford **(S)-10** (47.0 mg, 63%) as the TFA salt. ^{1}H NMR (400 MHz, DMSO-d_6) δ ppm 9.22 (s, 1H), 7.50 – 7.29 (m, 8H), 7.29 – 7.19 (m, 1H), 4.54 (s, 1H), 3.42 (d, J = 12.23 Hz, 2H), 3.18 – 3.09 (m, 2H), 3.04 (q, J = 11.21 Hz, 2H), 2.84 (d, J = 13.01 Hz, 2H), 2.21 (q, J = 11.50 Hz, 2H), 1.18 (t, J = 7.27 Hz, 3H); LCMS RT (Method 1) = 4.566 min; RT (Method 2) = 3.035 min, *m/z* 315.1 [M + H^+]; HRMS (ESI) *m/z* calcd for $C_{19}H_{24}ClN_2^+$ [M + H^+] 315.1623, found 315.1637.

bis(4-Chlorophenyl)methanol. A solution of **27** (3.00 g, 11.9 mmol) in MeOH (15.0 mL) was treated at 0 ^oC in portions with $NaBH_4$ (0.678 g, 17.9 mmol). The reaction mixture was stirred at 0 ^oC for 15 min, allowed to warm to room temperature and stirred for 2 h. The reaction was quenched with ice, diluted with H_2O and extracted with EtOAc. The organic layer was separated, dried over $MgSO_4$ and concentrated to give the title compound as a white solid (3.00 g, 99%), which was used without further purification. ^{1}H NMR (400 MHz, $CDCl_3$) δ ppm 7.31 (d, J = 8.8 Hz, 4H), 7.28 (d, J = 8.7 Hz, 4H), 5.78 (d, J = 3.2 Hz, 1H), 2.26 (d, J = 3.5 Hz, 1H). LCMS RT (Method 2) = 3.733 min, *m/z* 254.5 [M+H^+].

*4,4'-(Chloromethylene)bis(chlorobenzene) (**28**).* bis(4-Chlorophenyl)methanol (3.00 g, 11.8 mmol) was dissolved in CH_2Cl_2 (10.0 mL), to this was added 3-4 drops of DMF followed by thionyl chloride (2.60 mL, 35.6 mmol). The resulting reaction mixture was allowed to stir at room temperature for 45 min, after which TLC anlysis (20% EtOAc in Hex) showed completion. Reaction mixture was concentrated under reduced pressure to afford **28** (2.50 g, 78%) as a white solid, which was used without further purification. ^{1}H NMR (400 MHz, $CDCl_3$) δ ppm 7.42 – 7.27 (m, 8H), 6.06 (s, 1H). LCMS RT (Method 2) = 3.932 min, *m/z* 272.6 [M+H$^+$].

*1-(bis(4-Chlorophenyl)methyl)piperazine (**29**).* A solution of **28** (80.0 mg, 0.295 mmol) in THF (10.0 mL) was treated with piperazine (38.1 mg, 0.442 mmol) followed by K_2CO_3 (81.0 mg, 0.589 mmol). A catalytic amount of tetrabutylammonium iodide (10.9 mg, 0.029 mmol) was added to the mixture. The reaction mixture was refluxed for 8 h, after which LC/MS analysis showed completion. The reaction mixture was concentrated and re-disolved in EtOAc. The organic layer was washed three times with saturated $NaHCO_3$ solution, dried over $MgSO_4$, filtered and concentrated. The crude product was purified by preparative HPLC, to give **29** (80.0 mg, 63%) as the TFA salt. ^{1}H NMR (400 MHz, DMSO-d_6) δ ppm 8.50 (s, 2H), 7.43 (d, J = 8.7 Hz, 4H), 7.39 (d, J = 8.6 Hz, 4H), 4.56 (s, 1H), 3.11 (s, 4H), 2.46 (s, 4H). LCMS RT (Method 1) = 4.760 min, *m/z* 322.7 [M + H$^+$]; HRMS (ESI) *m/z* calcd for $C_{17}H_{19}Cl_2N_2^+$ [M + H$^+$] 321.0920, found 321.0930.

*1-(bis(4-Chlorophenyl)methyl)-4-methylpiperazine (**30**).* To a stirred solution of **28** (0.800 g, 2.95 mmol) in THF (10.0 mL) was added K_2CO_3 (0.814 g, 5.89 mmol), 1-methylpiperazine (0.654 mL, 5.89 mmol) and catalytic potassium iodide (73.0 mg, 0.442 mmol). The reaction was heated to 100 ^{o}C for 48 h. The reaction mixture was partitioned between EtOAc and H_2O, the layers separated and the organic phase washed with brine, dried over $MgSO_4$, filtered and

concentrated. Crude mixture was purified by flash column chromatography: silica gel with a gradient of 0-5% MeOH in CH_2Cl_2 to afford **30** (603 mg, 61%) as a free-base oil, which was then mixed in a 1:1 ratio with oxalic acid to form the oxalate salt as a white powder. ^{1}H NMR (400 MHz, DMSO-d_6) δ ppm 7.41 (d, J = 8.6 Hz, 4H), 7.34 (d, J = 8.5 Hz, 4H), 4.33 (s, 1H), 2.32 (s, 4H), 2.27 (s, 4H), 2.14 (s, 3H). LCMS RT (Method 1) = 4.843 min,

m/z 336.9 [M + H^+]; HRMS (ESI) *m/z* calcd for $C_{18}H_{21}Cl_2N_2^+$ [M + H^+] 335.1076, found 335.1086.

*1-(bis(4-Chlorophenyl)methyl)-4-ethylpiperazine, (**31**).* A solution of **28** (160 mg, 0.589 mmol) in THF (10.0 mL) was treated with 1-ethylpiperazine (101 mg, 0.884 mmol) followed by K_2CO_3 (163 mg, 1.18 mmol). A catalytic amount of tetrabutylammonium iodide (21.8 mg, 0.059 mmol) was added, and the resulting reaction mixture was heated to 100 ^{o}C for 48 hours. The reaction mixture was partitioned between EtOAc and H_2O, the layers separated and the organic phase washed with brine, dried over $MgSO_4$, filtered and concentrated. Crude mixture was purified by flash column chromatography: silica gel with a gradient of 0-5% MeOH in CH_2Cl_2 to afford **31** (123 mg, 60%) as a free-base oil, which was then mixed in a 1:1 ratio with oxalic acid to form the oxalate salt. ^{1}H NMR (400 MHz, DMSO-d_6) δ ppm 7.44 (d, J = 8.8 Hz, 4H), 7.40 (d, J = 8.8 Hz, 4H), 4.57 (s, 1H), 3.11 – 3.02 (m, 2H), 2.80 (s, 8H), 2.24 (s, 2H), 1.17 (t, J = 7.2 Hz, 3H). LCMS RT (Method 1) = 5.029 min,

m/z 350.7 [M + H^+]; HRMS (ESI) *m/z* calcd for $C_{19}H_{23}Cl_2N_2^+$ [M + H^+] 349.1233, found 349.1239.

2-(2-(2-(4-((4-Chlorophenyl)(phenyl)methyl)piperazin-1-yl)ethoxy)ethyl)isoindoline-1,3-dione ***(Rac-22)***. Et_3N (0.279 mL, 2.00 mmol) was added to a solution of **Rac-5** (250 mg, 0.667 mmol) in THF (10.0 mL) at room temperature. The mixture was stirred for 15 min, then phthalimide (147 mg, 1.000 mmol) and triphenylphosphine (262 mg, 1.00 mmol) were added to the mixture followed by diisopropyl azodicarboxylate (0.130 mL, 0.667 mmol). The reaction mixture was stirred at room temperature for 4 h, after which LCMS analysis showed product formation. Reaction mixture was concentrated to dryness and residue purified by preparative HPLC to give **Rac-22** (239 mg, 58%) as the TFA salt. ^{1}H NMR (400 MHz, DMSO-d_6) δ ppm 9.42 (s, 1H), 7.72 (m, 4H), 7.46 (d, J = 8.4 Hz, 2H), 7.44 – 7.38 (m, 4H), 7.34 (t, J = 7.5 Hz, 2H), 7.25 (t, J = 7.4 Hz, 1H), 4.53 (s, 1H), 3.73 (d, J = 4.8 Hz, 4H), 3.58 (t, J = 5.2 Hz, 4H), 3.14 (d, J = 11.2 Hz, 2H), 3.04 – 2.97 (m, 2H), 2.82 (d, J = 12.8 Hz, 2H), 2.28 (m, 2H). LCMS RT (Method 1) = 5.205 min, *m/z* 505.7 [M + H^+]; HRMS (ESI) *m/z* calcd for $C_{29}H_{31}ClN_3O_3^+$ [M + H^+] 504.2048, found 504.2043.

2-(2-(4-((4-Chlorophenyl)(phenyl)methyl)piperazin-1-yl)ethoxy)ethanamine ***(Rac-23)***. Hydrazine (0.181 mL, 5.77 mmol) was added to a solution of **Rac-22 (**97.0 mg, 0.192 mmol) in EtOH (3.00 mL). The reaction mixture was stirred at 60 °C for 3 h, after which LCMS analysis showed completion. The reaction mixture was concentrated under reduced pressure and residue purified by preparative HPLC, to give **Rac-23** (58.0 mg, 63%) as the TFA salt. ^{1}H NMR (400 MHz, DMSO-d_6) δ ppm 9.39 (s, 1H), 7.44 (d, J = 8.1 Hz, 2H), 7.41 – 7.38 (m, 4H), 7.35 (t, J = 7.8 Hz, 2H), 7.23 (t, J = 7.3 Hz, 1H), 4.55 (s, 1H), 3.77 (d, J = 4.6 Hz, 2H), 3.55 (t, J = 5.0 Hz, 4H), 3.19 (d, J = 11.0 Hz, 2H), 3.09 – 2.95 (m, 2H), 2.80 (d, J = 11.5 Hz, 2H), 2.25 (m, 2H). LCMS RT (Method 1) = 3.959 min,

m/z 374.7 [M + H^+]; HRMS (ESI) *m/z* calcd for $C_{21}H_{29}ClN_3O^+$ [M + H^+] 374.1994, found 374.2002.

*tert-Butyl (14-(4-((4-chlorophenyl)(phenyl)methyl)piperazin-1-yl)-3,6,9,12-tetraoxatetradecyl)carbamate (**Rac-24**).* A solution of **Rac-5** (250 mg, 0.558 mmol) in DMF (5.00 mL) was treated with a 60% dispersion in mineral oil of NaH (89.0 mg, 2.23 mmol) at 0 ^oC. The reaction mixture was stirred at 0 ^oC for 10 min and room temperature for 30 min. To this mixture was added a solution of tert-butyl (2-(2-(2-bromoethoxy)ethoxy)ethyl)carbamate (174 mg, 0.558 mmol) in DMF (1.00 mL) and the resulting mixture allowed to stir overnight. The mixture was quenched with H_2O and extracted with CH_2Cl_2. The organic layer was separated, dried over $MgSO_4$, filtered and concentrated. Crude residue was purified by preparative HPLC, to give **Rac-24** (220 mg, 55%) as the TFA salt. ^1H NMR (400 MHz, $CDCl_3$) δ ppm 7.45 – 7.37 (m, 4H), 7.37 – 7.18 (m, 5H), 4.44 (s, 1H), 3.86 (t, J = 4.4 Hz, 2H), 3.63 – 3.48 (m, 14H), 3.29 (s, 4H), 2.91 (s, 9H), 1.43 (s, 9H). ^{19}F NMR (376 MHz, $CDCl_3$) δ ppm -75.78. LCMS RT (Method 1) = 5.372 min,

m/z 607.7 [M + H^+]; HRMS (ESI) *m/z* calcd for $C_{32}H_{49}ClN_3O_6^+$ [M + H^+] 606.3304, found 606.3307.

*14-(4-((4-Chlorophenyl)(phenyl)methyl)piperazin-1-yl)-3,6,9,12-tetraoxatetradecan-1-amine (**Rac-25**).* A solution of **Rac-24** (217 mg, 0.358 mmol) in CH_2Cl_2 (10.0 mL) was treated with trifluoroacetic acid (5.00 mL) at 0 ^oC. The reaction mixture was stirred at 0 ^oC for 10 min and room temperature for 30 min, after which LCMS analysis showed completion. The reaction mixture was concentrated and the crude residue was purified by preparative HPLC, to give **Rac-25** (109 mg, 60%) as the TFA salt. ^1H NMR (400 MHz, $CDCl_3$) δ ppm 7.95 (s, 2H), 7.51 – 7.41

(m, 4H), 7.38 – 7.25 (m, 4H), 4.57 (s, 1H), 3.79 (dd, J = 11.2, 6.6 Hz, 4H), 3.70 – 3.49 (m, 9H), 3.58 (s, 7H), 3.36 (d, J = 4.8 Hz, 2H), 3.17 (s, 3H), 3.00 (s, 5H). ^{19}F NMR (376 MHz, $CDCl_3$) δ -75.78. LCMS RT (Method 1) = 3.916 min,

m/z 507.2 [M + H^+]; HRMS (ESI) *m/z* calcd for $C_{27}H_{41}ClN_3O_4^+$ [M + H^+] 506.2780, found 506.2803.

Cells and viruses. Human hepatoma cell line Huh7.5.1 and other Huh7-derived cells were maintained in Dulbecco's modified Eagle's medium (DMEM) (Life technologies, Grand Island, NY, USA) with 10% fetal bovine serum (FBS) (Life technologies, Grand Island, NY, USA) and antibiotics in 5% CO_2 at 37°C. HCV-Luc (HCV JFH-1 strain with insertion of the luciferase reporter gene) and pseudotyped viruses (HCVpp-1a, HCVpp-1b and VSV-Gpp) were produced as reported before. HCV-Luc (HCV JFH-1 strain with insertion of the luciferase reporter gene), HCVsc (single-round infectious defective HCV particle) and pseudotyped viruses (HCVpp-1a, HCVpp-1b and VSV-Gpp) were produced as reported before.[13, 22]

HCV-Luc infection and ATPlite assays. Huh7.5.1 cells were plated in 96-well plates at 10^4 cells/well and incubated overnight. The cells were infected with HCV-Luc in the presence of increasing concentration of compound of interest. Viral level was measured 48 h after treatment using *Renilla* Luciferase assay system (Promega, Madison, WI, USA). ATP-based cell viability assay was carried out in parallel to evaluate the cytotoxicity with ATPlite assay kit (PerkinElmer, Waltham, MA, USA). The concentration values that lead to 50% viral inhibition and cytotoxicity (EC_{50} and CC_{50}) were calculated using nonlinear regression equation in GraphPad Prism 5.0 software (GraphPad Software Inc., La Jolla, CA, USA).

HCV Replication cycle assays. In HCVsc assay, Huh7.5.1 cells that were cultured in 96-well plates (10^4 cells/well) overnight before infection with HCVsc in the presence of compound

treatments. After 48 h of incubation, the viral level was detected by a luciferase assay, In HCV subgenomic replicon assay, HCV replicon (GT 2a) cells were plated into 96-well plate at 10^4 cells/well and incubated overnight. The cells were treated with tested compounds for 48 h and luciferase activity was measured. In HCVpp assays, Huh7.5.1 cells were seeded in 96-well plates (10^4 cells/well) and cultured overnight. Then the cells were infected with HCVpp GT 1a, 1b, VSV-Gpp and MLVpp for 4 h in the present of compound treatment. The cells were then washed and cultured for 48 h followed by a luciferase assay to detect the HCV entry. Positive controls (cyclosporin A at 10 μM and bafilomycin A1 at 10 nM) were tested in parallel.

H1HR inhibition assay. PathHunter β-Arrestin GPCR assay kit (DiscoveRx, Fremont, CA, USA) was used following the antagonist procedure. The PathHunter cells were plated in white 96-well plates with clear bottom and cultured overnight. After incubation with the compound of interest for 3 h, agonist histamine at 0.25 μM were added and plates were incubated for additional 2 h. Chemiluminescent signal was read after 60 min incubation with detection agent at room temperature. %Anti-histamine activity was calculated based on the result from histamine-treated wells.

DENV-RVPs assay and NIAID screen. Huh7.5.1 cells were plated in 96-well plates at 10^4 cells/well and cultured overnight. Dengue RVPs (Integral Molecular, Philadelphia, PA, USA) was added to the cells with increasing concentrations of compound of interest. Dengue RVP reproducibility was measured by luciferase signal 48 h after treatment. Lycorine HCl was tested as positive control.[33, 34] The non-clinical and pre-clinical services program offered by the National Institute of Allergy and Infectious Diseases (NIAID) (http://www.niaid.nih.gov/labsandresources/resources/dmid/invitro/Pages/invitro.aspx) was used for antiviral screen against the 13 viruses. The viruses include hepatitis B virus, HCV replicon,

herpes simplex virus-1, human cytomegalovirus, vaccinia virus, dengue virus, influenza A (H1N1) virus, respiratory syncytial virus, SARS coronavirus, poliovirus 3, Rift Valley fever virus, Tacaribe virus, and Venezuelan equine encephalitis virus.

***In vitro* and *In vivo* pharmacokinetics properties.** The in vitro microsomal stability was measured by incubation of compounds with human/mouse/rat liver microsomes at 37°C in the presence of the co-factor, NADPH. The concentrations of compounds were measured by LC-MS/MS at 0, 5, 15, 30 and 45 minutes. half-life ($t_{1/2}$) was calculated as described before [35].

The kinetic solubility of compounds was determined in phosphate buffer pH 7.4, using μSOL Evolution from pION Inc. (www.pion-inc.com), with a fully automated system of sample preparation, sample analysis and data processing. The effective permeability of compounds was determined via passive diffusion using stirring double-sink PAMPA (Parallel Artificial Membrane Permeability Assay) method from pION Inc. (www.pion-inc.com), with a fully automated system of sample preparation, sample analysis and data processing.

For *in vivo* pharmacokinetics, twenty-seven male CD-1 mice (~35 g) were obtained from Charles River Laboratories (Wilmington, MA). Mice were housed at the centralized animal facilities at the NIH (Bethesda, MD) with a 12 h light dark cycle. The housing temperature and relative humidity were controlled at 22°C and 55%, respectively. The animals had free access to water and food. All experimental procedures were approved by the Animal Ethics Committee of the NIH. A dosing concentration of 2 mg/mL of the appropriate compound was freshly prepared in 50% PEG300 and 50% water. The pharmacokinetics was evaluated after single intraperitoneal administration at 10 mg/kg. The blood and liver samples were collected at predose, 0.083, 0.25, 0.5, 1, 2, 4, 7 and 24 hr. Three samples (n = 3) were collected at each time point. The concentrations of compound in plasma and liver were determined by ultra-performance liquid

chromatography-mass spectrometry analysis (UPLC-MS/MS. The pharmacokinetic parameters were calculated using the non-compartmental method (Model 200) of the pharmacokinetic software package Phoenix WinNonlin, version 6.2 (Certara, St. Louis, MO, USA). The area under the plasma and liver concentration versus time curve (AUC) was calculated using the linear trapezoidal method. Where warranted, the slope of the apparent terminal phase was estimated by log linear regression using at least 3 data points and the terminal rate constant (λ) was derived from the slope. $AUC_{0-\infty}$ was estimated as the sum of the AUC_{0-t} (where t is the time of the last measurable concentration) and $C_{t/\lambda}$. The apparent terminal half-life ($t_{½}$) was calculated as $0.693/\lambda$.

ASSOCIATED CONTENT

Supporting Information

Antiviral activity of CCZ analogues against dengue virus, general chemistry methods and compound characterization are included. This material is available free of charge via the Internet at http://pubs.acs.org.

AUTHOR INFORMATION

Corresponding Author

*For T.J.L.: phone, 301-496-1721; fax, 301-402-1612; E-mail, jliang@nih.gov. For J.J.M.: phone, 301-217-9198; fax, 301-217-5736; E-mail: maruganj@mail.nih.gov.

Present Addresses

†If an author's address is different than the one given in the affiliation line, this information may be included here.

Author Contributions

The manuscript was written through contributions of all authors. All authors have given approval to the final version of the manuscript. §These authors contributed equally.

Funding Sources

The Intramural Research Program of the National Institute of Diabetes and Digestive and Kidney Diseases and Molecular libraries funding.

Notes

T.J.L, M.F., S.H, X.H, Z.H, J.J.M., J.X., and W.Z are named as inventors on patent applications related to this work: U.S. Provisional Patent Appl. 62/011,462, "Heterocyclic compounds and methods of use thereof". Other authors declare no competing interests.

ACKNOWLEDGMENT

We thank S. Michael and M. Balcom for assistance in robotic control in qHTS; P. Shinn, M. Itkin, and D. van Leer for help with compound management; and B. Zhang for technical assistance.

ABBREVIATIONS USED

HCV, Hepatitis C virus; IFN-α, interferon α; RBV, ribavirin; DAAs, direct-acting antivirals; HTAs, Host-targeting agents; NPC, NCGC Pharmaceutical Collection; qHTS, high-throughput screening; CCZ, chlorcylizine HCl; SAR, structure-activity relationship; DMSO, dimethyl sulfoxide; HCV-Luc, HCV JFH-1 strain with insertion of the luciferase reporter gene; EC_{50}, the concentration of compound that inhibited 50% of virus level of DMSO; $CC_{50,}$ the concentration of compound that exhibited 50% of cytotoxicity of DMSO; H1HR, H1-histamine receptor; HCVsc, single-round infectious defective HCV particles; HCVpp, HCV pseudoparticle; ADME, absorption, distribution, metabolism, and excretion; i.p., intraperitoneal; DMF, *N*,*N*-dimethylformamide; LC/MS, liquid chromatography–mass spectrometry; TOF, Time-of-Flight; TFA, trifluoroacetic acid; SFC, supercritical fluid chromatography; THF, tetrahydrofuran;

DMEM, Dulbecco's modified Eagle's medium; FBS, fetal bovine serum; NIAID, National Institute of Allergy and Infectious Diseases.

REFERENCES

1. Scheel, T. K. H.; Rice, C. M. Understanding the Hepatitis C Virus Life Cycle Paves the Way for Highly Effective Therapies. *Nat. Med.* **2013,** *19*, 837-849.

2. Liang, T. J.; Ghany, M. G. Current and Future Therapies for Hepatitis C Virus Infection. *N. Engl. J. Med.* **2013,** *368*, 1907-1917.

3. Liang, T. J. Current Progress in Development of Hepatitis C Virus Vaccines. *Nat. Med.* **2013,** *19*, 869-878.

4. Liang, T. J.; Rehermann, B.; Seeff, L. B.; Hoofnagle, J. H. Pathogenesis, Natural History, Treatment, and Prevention of Hepatitis C. *Ann. Intern. Med.* **2000,** *132*, 296-305.

5. Thomas, D. L. Global Control of Hepatitis C: Where Challenge Meets Opportunity. *Nat. Med.* **2013,** *19*, 850-858.

6. Afdhal, N.; Reddy, K. R.; Nelson, D. R.; Lawitz, E.; Gordon, S. C.; Schiff, E.; Nahass, R.; Ghalib, R.; Gitlin, N.; Herring, R.; Lalezari, J.; Younes, Z. H.; Pockros, P. J.; Di Bisceglie, A. M.; Arora, S.; Subramanian, G. M.; Zhu, Y.; Dvory-Sobol, H.; Yang, J. C.; Pang, P. S.; Symonds, W. T.; McHutchison, J. G.; Muir, A. J.; Sulkowski, M.; Kwo, P. Ledipasvir and Sofosbuvir for Previously Treated HCV Genotype 1 Infection. *N. Engl. J. Med.* **2014,** *370*, 1483-1493.

7. Afdhal, N.; Zeuzem, S.; Kwo, P.; Chojkier, M.; Gitlin, N.; Puoti, M.; Romero-Gomez, M.; Zarski, J. P.; Agarwal, K.; Buggisch, P.; Foster, G. R.; Brau, N.; Buti, M.; Jacobson, I. M.;

Subramanian, G. M.; Ding, X.; Mo, H.; Yang, J. C.; Pang, P. S.; Symonds, W. T.; McHutchison, J. G.; Muir, A. J.; Mangia, A.; Marcellin, P. Ledipasvir and Sofosbuvir for Untreated HCV Genotype 1 Infection. *N. Engl. J. Med.* **2014,** *370*, 1889-1898.

8. Conteduca, V.; Sansonno, D.; Russi, S.; Pavone, F.; Dammacco, F. Therapy of Chronic Hepatitis C Virus Infection in the Era of Direct-Acting and Host-Targeting Antiviral Agents. *J. Infect.* **2014,** *68*, 1-20.

9. Sofia, M. J.; Bao, D.; Chang, W.; Du, J.; Nagarathnam, D.; Rachakonda, S.; Reddy, P. G.; Ross, B. S.; Wang, P.; Zhang, H. R.; Bansal, S.; Espiritu, C.; Keilman, M.; Lam, A. M.; Steuer, H. M.; Niu, C.; Otto, M. J.; Furman, P. A. Discovery of a β-D-2'-Deoxy-2'-α-fluoro-2'-β-*C*-methyluridine Nucleotide Prodrug (PSI-7977) for the Treatment of Hepatitis C Virus. *J. Med. Chem.* **2010,** *53*, 7202-7218.

10. Callaway, E. Hepatitis C Drugs not Reaching Poor. *Nature* **2014,** *508*, 295-296.

11. Zeuzem, S. Decade in Review - HCV: Hepatitis C Therapy - A Fast and Competitive Race. *Nat. Rev. Gastroenterol. Hepatol.* **2014,** *11*, 644-645.

12. Puyang, X.; Poulin, D. L.; Mathy, J. E.; Anderson, L. J.; Ma, S.; Fang, Z.; Zhu, S.; Lin, K.; Fujimoto, R.; Compton, T.; Wiedmann, B. Mechanism of Resistance of Hepatitis C Virus Replicons to Structurally Distinct Cyclophilin Inhibitors. *Antimicrob. Agents Chemother.* **2010,** *54*, 1981-1987.

13. Hu, Z.; Lan, K. H.; He, S.; Swaroop, M.; Hu, X.; Southall, N.; Zheng, W.; Liang, T. J. Novel Cell-Based Hepatitis C Virus Infection Assay for Quantitative High-Throughput Screening of Anti-Hepatitis C Virus Compounds. *Antimicrob. Agents Chemother.* **2014,** *58*, 995-1004.

14. He, S.; Lin, B.; Chu, V.; Hu, Z.; Hu, X.; Xiao, J.; Wang, A. Q.; Schweitzer, C. J.; Li, Q.; Imamura, M.; Hiraga, N.; Southall, N.; Ferrer, M.; Zheng, W.; Chayama, K.; Marugan, J. J.; Liang, T. J. Repurposing of the Antihistamine Chlorcyclizine and Related Compounds for Treatment of Hepatitis C Virus Infection. *Sci. Transl. Med.* **2015,** *7*, 282ra49.

15. Huang, R.; Southall, N.; Wang, Y.; Yasgar, A.; Shinn, P.; Jadhav, A.; Nguyen, D. T.; Austin, C. P. The NCGC Pharmaceutical Collection: A Comprehensive Resource of Clinically Approved Drugs Enabling Repurposing and Chemical Genomics. *Sci. Transl. Med.* **2011,** *3*, 80ps16.

16. Chamoun-Emanuelli, A. M.; Pecheur, E. I.; Chen, Z. Benzhydrylpiperazine Compounds Inhibit Cholesterol-Dependent Cellular Entry of Hepatitis C Virus. *Antiviral Res.* **2014,** *109*, 141-148.

17. Mattson, R. J.; Pham, K. M.; Leuck, D. J.; Cowen, K. A. An Improved Method for Reductive Alkylation of Amines using Titanium(IV) Isopropoxide and Sodium Cyanoborohybride. *J. Org. Chem.* **1990,** *55*, 2552-2554.

18. Kuntzman, R.; Phillips, A.; Tsai, I.; Klutch, A.; Burns, J. J. *N*-Oxide Formation: A New Route for Inactivation of the Antihistaminic Chlorcyclizine. *J. Pharmacol. Exp. Ther.* **1967,** *155*, 337-344.

19. Gaertner, H. J.; Breyer, U.; Liomin, G. Chronic Administration of Chlorcyclizine and Meclizine to Rats: Accumulation of a Metabolite Formed by Piperazine Ring Cleavage. *J. Pharmacol. Exp. Ther.* **1973,** *185*, 195-201.

20. Dumasia, M. C.; Grainger, L.; Houghton, E. Biotransformation of Cyclizine in Greyhounds. 1: Identification and Analysis of Cyclizine and Some Basic Metabolites in Canine Urine by Gas Chromatography-Mass Spectrometry. *Xenobiotica* **2002,** *32*, 795-807.

21. Criado, P. R.; Criado, R. F.; Maruta, C. W.; Machado Filho, C. Histamine, Histamine Receptors and Antihistamines: New Concepts. *An. Bras. Dermatol.* **2010,** *85*, 195-210.

22. Hsu, M.; Zhang, J.; Flint, M.; Logvinoff, C.; Cheng-Mayer, C.; Rice, C. M.; McKeating, J. A. Hepatitis C Virus Glycoproteins Mediate pH-Dependent Cell Entry of Pseudotyped Retroviral Particles. *Proc. Natl. Acad. Sci. U S A* **2003,** *100*, 7271-7276.

23. He, J.; Choe, S.; Walker, R.; Di Marzio, P.; Morgan, D. O.; Landau, N. R. Human Immunodeficiency Virus Type 1 Viral Protein R (Vpr) Arrests Cells in the G2 Phase of the Cell Cycle by Inhibiting p34cdc2 Activity. *J. Virol.* **1995,** *69*, 6705-6711.

24. Chang, L. J.; Urlacher, V.; Iwakuma, T.; Cui, Y.; Zucali, J. Efficacy and Safety Analyses of a Recombinant Human Immunodeficiency Virus Type 1 Derived Vector System. *Gene Ther.* **1999,** *6*, 715-728.

25. Liu, S.; McCormick, K. D.; Zhao, W.; Zhao, T.; Fan, D.; Wang, T. Human Apolipoprotein E Peptides Inhibit Hepatitis C Virus Entry by Blocking Virus Binding. *Hepatology* **2012,** *56*, 484-491.

26. Sainz, B., Jr.; Barretto, N.; Martin, D. N.; Hiraga, N.; Imamura, M.; Hussain, S.; Marsh, K. A.; Yu, X.; Chayama, K.; Alrefai, W. A.; Uprichard, S. L. Identification of the Niemann-Pick C1-Like 1 Cholesterol Absorption Receptor as a New Hepatitis C Virus Entry Factor. *Nat. Med.* **2012,** *18*, 281-285.

27. Smith, B. D.; Morgan, R. L.; Beckett, G. A.; Falck-Ytter, Y.; Holtzman, D.; Teo, C.-G.; Jewett, A.; Baack, B.; Rein, D. B.; Patel, N.; Alter, M.; Yartel, A.; Ward, J. W.; Centers for Disease, C.; Prevention. Recommendations for the Identification of Chronic Hepatitis C Virus Infection Among Persons Born During 1945-1965. *MMWR. Recommendations and Reports :*

Morbidity and Mortality Weekly Report. Recommendations and Reports / Centers for Disease Control **2012,** *61*, 1-32.

28. Wang, L.; Jiang, H.; Zhou, Y.; Liu, B.; Ji, Z. Synthesis and Antiallergic Activities of Diphenylmethylpiperazine Derivatives. *Zhongguo Yaowu Huaxue Zazhi* **2002,** *12*, 125-129.

29. Younes, S.; Baziard-Mouysset, G.; de Saqui-Sannes, G.; Stigliani, J. L.; Payard, M.; Bonnafous, R.; Tisne-Versailles, J. Synthesis and Pharmacological Study of New Calcium Antagonists, Analogs of Cinnarizine and Flunarizine. *Eur. J. Med. Chem.* **1993,** *28*, 943-948.

30. Baltzly, R.; DuBreuil, S.; Ide, W. S.; Lorz, E. Unsymmetrically Disubstituted Piperazines. III. N-Methyl-N'-benzhydrylpiperazines as Histamine Antagonists. *J. Org. Chem.* **1949,** *14*, 775-782.

31. Phan, T. B.; Nolte, C.; Kobayashi, S.; Ofial, A. R.; Mayr, H. Can One Predict Changes from S(N)1 to S(N)2 Mechanisms? *J. Am. Chem. Soc.* **2009,** *131*, 11392-11401.

32. Morren, H. G.; Denayer, R.; Linz, R.; Mathieu, J.; Strubbe, H.; Trolin, S. New Derivatives of 1,4-Disubstituted Piperazine. *Industrie Chimique Belge* **1957,** *22*, 409-420.

33. Wang, P.; Li, L. F.; Wang, Q. Y.; Shang, L. Q.; Shi, P. Y.; Yin, Z. Anti-Dengue-Virus Activity and Structure-Activity Relationship Studies of Lycorine Derivatives. *ChemMedChem* **2014,** *9*, 1522-1533.

34. Qing, M.; Liu, W.; Yuan, Z.; Gu, F.; Shi, P. Y. A High-Throughput Assay using Dengue-1 Virus-Like Particles for Drug Discovery. *Antiviral Res.* **2010,** *86*, 163-171.

35. Obach, R. S. Prediction of Human Clearance of Twenty-Nine Drugs from Hepatic Microsomal Intrinsic Clearance Data: An Examination of *in vitro* Half-Life Approach and Nonspecific Binding to Microsomes. *Drug Metab. Dispos.* **1999,** *27*, 1350-1359.

TABLES

Table 1. Structural modifications with substituents on the piperazine ring[a]

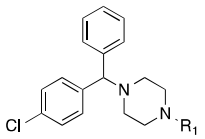

Compd	R_1	EC_{50} (μ M) [a]	CC_{50} (μ M) [a]	Selectivity Index	Compd	R_1	EC_{50} (μ M) [a]	CC_{50} (μ M) [a]	Selectivity Index
Rac-2		0.044 ± 0.011	49.8 ± 17.2	1132	**(S)-19**		22.0 ± 3.2	91.3 ± 1.0	4
(S)-2		0.024 ± 0.009	33.4 ± 2.4	1392	**(S)-14**	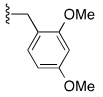	0.456 ± 0.235	38.4 ± 4.2	84
(R)-2		0.020 ± 0.005	37.5 ± 4.2	1875	**(S)-20**		0.063 ± 0.025	77.9 ± 3.1	1237
Rac-1		0.035 ± 0.013	10.4 ± 0.2	297	**(R)-20**		0.040 ± 0.017	46.7 ± 0.4	1168
(S)-1		0.032 ± 0.007	9.31 ± 0.04	333	**(S)-15**		0.036 ± 0.015	71.3 ± 11.4	1981
(R)-1		0.032 ± 0.022	12.5 ± 1.4	391	**(R)-15**		0.035 ± 0.008	81.5 ± 0.5	2329
(S)-10		0.027 ± 0.005	40.0 ± 1.1	1600	**(S)-21**		> 31.6	> 100	N/A
(R)-10		0.0099 ± 0.0054	37.9 ± 3.3	3828	**(R)-21**		> 31.6	> 100	N/A
(S)-11		0.032 ± 0.018	39.7 ± 0.9	1241	**Rac-3**	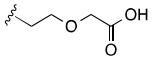	> 31.6	> 100	N/A
(R)-11		0.024 ± 0.005	48.5 ± 1.1	2021	**Rac-4**	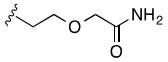	0.103 ± 0.052	> 100	> 910
(S)-18		0.013 ± 0.004	32.4 ± 3.8	2492	**Rac-22**	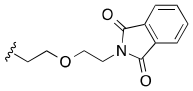	1.54 ± 0.57	> 100	> 65
(S)-12		0.042 ± 0.023	31.1 ± 4.2	740	**Rac-24**	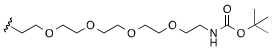	0.199 ± 0.030	19.0 ± 4.0	95
(R)-12		0.195 ± 0.084	40.8 ± 0.4	209	**Rac-26**	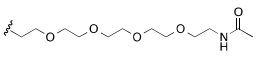	0.170 ± 0.022	> 100	> 588
(S)-13		0.102 ± 0.018	51.7 ± 1.4	507	**Rac-5**	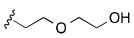	0.032 ± 0.011	42.6 ± 1.8	1331
(R)-13		0.232 ± 0.061	58.2 ± 7.2	251	**Rac-23**	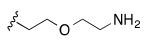	0.0072 ± 0.0018	8.18 ± 0.40	1152
(S)-16		0.019 ± 0.006	30.4 ± 2.8	1600	**Rac-25**	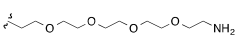	0.028 ± 0.007	12.2 ± 0.8	436
(S)-17		0.177 ± 0.037	12.3 ± 0.3	69					

[a] EC_{50} ± SEM ($n \geq 3$) is from HCV-Luc infection assay; CC_{50} ± SEM ($n \geq 3$) is from ATPlite cytotoxicity assay; Selective index = CC_{50}/ EC_{50}.

Table 2. Structural modifications on the phenyl rings [a]

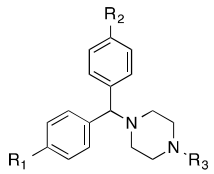

Compd	R_1	R_2	R_3	EC_{50} (μM) [a]	CC_{50} (μM) [a]	Selectivity Index
Rac-2	Cl	H		0.044 ± 0.011	49.8 ± 17.2	1132
6	H	H		1.14 ± 0.37	> 100	> 88
30	Cl	Cl		0.017 ± 0.005	21.3 ± 2.3	1253
Rac-1	Cl	H		0.035 ± 0.013	10.4 ± 0.2	297
29	Cl	Cl		0.033 ± 0.007	5.64 ± 0.80	201
Rac-36	Br	H		0.063 ± 0.014	7.93 ± 0.83	126
Rac-37	Cl	Br		0.010 ± 0.004	2.26 ± 0.29	226
(S)-10	Cl	H		0.027 ± 0.005	40.0 ± 1.1	2000
31	Cl	Cl		0.0023 ± 0.0007	19.8 ± 1.9	8609
Rac-38	Br	H		0.0070 ± 0.0004	35.2 ± 1.4	5029
Rac-39	Cl	Br		0.0040 ± 0.0016	21.7 ± 3.4	5425
Rac-5	Cl	H	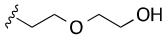	0.032 ± 0.011	42.6 ± 1.8	1331
34	Cl	Cl	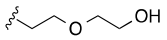	0.012 ± 0.003	19.7 ± 2.4	1990
Rac-25	Cl	H	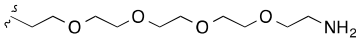	0.028 ± 0.007	12.2 ± 0.8	436
35	Cl	Cl	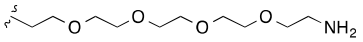	0.014 ± 0.001	4.43 ± 0.12	316

[a] EC_{50} ± SEM ($n \geq 3$) is from HCV-Luc infection assay; CC_{50} ± SEM ($n \geq 3$) is from ATPlite cytotoxicity assay; Selectivity index = CC_{50}/ EC_{50}.

Table 3. Structural modifications within the piperazine core[a]

Compd	Structure	EC_{50} (μ M) [a]	CC_{50} (μ M) [a]	Selectivity Index	Compd	Structure	EC_{50} (μ M) [a]	CC_{50} (μ M) [a]	Selectivity Index
Rac-2	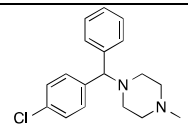	0.044 ± 0.011	49.8 ± 17.2	1132	**6**	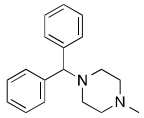	1.14 ± 0.37	> 100	> 88
Rac-7	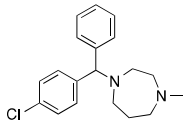	0.057 ± 0.008	12.8 ± 0.1	225	**44**	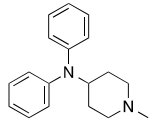	2.72 ± 1.13	56.8 ± 8.2	21
29	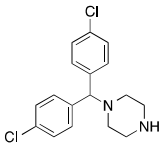	0.033 ± 0.007	5.64 ± 0.80	201	**45**	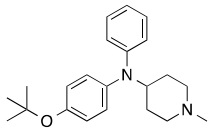	0.354 ± 0.097	78.7 ± 0.6	222
32	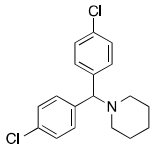	17.4 ± 2.8	69.0 ± 0.9	4	**8**	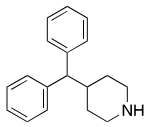	0.072 ± 0.002	32.5 ± 0.1	451
33	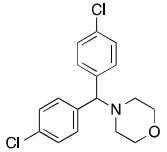	29.7 ± 0.1	62.1 ± 2.8	2	**9**	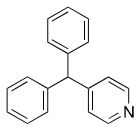	> 31.6	65.1 ± 2.1	< 2
Rac-38	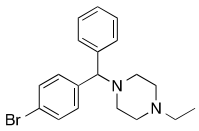	0.0070 ± 0.0004	35.2 ± 1.4	5029	**48**	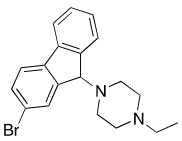	1.68 ± 0.42	53.1 ± 1.3	32

[a] EC_{50} ± SEM ($n \geq 3$) is from HCV-Luc infection assay; CC_{50} ± SEM ($n \geq 3$) is from ATPlite cytotoxicity assay; Selectivity index = CC_{50}/EC_{50}.

Table 4. Anti-HCV, metabolic and physical properties profile of selected analogues

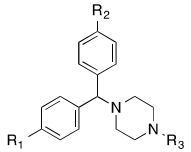

Compd	Chemical structure				Anti-HCV activity and selectivity[a]						HCV replication cycle assays[b]						Other properties				
	R1	R2	R3	Salt	EC_{50} (μM)	CC_{50} (μM)			Selectivity Index	H1HR[c] %DMSO at 10 nM	HCVsc[c] %DMSO	HCVpp[c] %DMSO		MLVpp[c] %DMSO	VSV-Gpp[c] %DMSO	Replicon[c] %DMSO	Microsomal $t_{1/2}$ (min)			Permeability (10^{-6} cm/s)	Solubility (μg/mL)
						Huh7.5.1	HepG2	Primary human hepatocyte				GT 1a	GT 1b			GT 2a	Human	Mouse	Rat		
Rac-2	Cl	H		TFA	0.044	49.8	-	-	1132	16.0	24.9	92.5	120	124	105	102	113	36	4.6	-	-
(S)-2	Cl	H		TFA	0.024	33.4	32.3	> 31.6	1392	49.5	2.1	107	116	103	120	101	-	-	-	1834	29.3
(S)-1	Cl	H		-	0.032	9.31	-	9.01	291	88.1	28.1	98.8	66.3	57.5	51.9	61.5	-	-	-	> 1920.0	30.3
(S)-10	Cl	H		TFA	0.027	40.0	68.9	> 31.6	1481	60.7	2.0	-	-	-	-	-	-	-	-	514.5	12.3
Rac-23	Cl	H	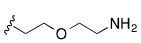	TFA	0.0072	8.18	6.17	8.98	1136	21.5	6.9	19.4	37.2	107	93.1	149	26.3	25	12.2	-	44.3
Rac-25	Cl	H	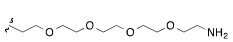	TFA	0.028	12.2	12.6	9.39	436	54.1	1.4	95.8	91.7	117	99.8	63.6	26.2	29.1	11.7	682.1	46
30	Cl	Cl		TFA	0.017	21.3	31.6	> 31.6	1253	18.5	12.4	76.2	91.9	116	119	112	>120	91	26	1024.3	> 49.0
29	Cl	Cl		TFA	0.033	5.64	4.28	4.18	171	90.8	10.2	107	137	120	115	147	>30	17.3	20.7	-	19.9
31	Cl	Cl		TFA	0.0023	19.8	56.0	24.3	8609	31.7	10.1	76.6	108	96.5	110	128	~30	12.6	2.20	892.3	17.7
34	Cl	Cl		TFA	0.013	19.7	19.5	> 31.6	1515	23.7	1.8	71.7	80.8	108	109	98.8	>30	10	13.7	-	44.5

[a] EC_{50} ± SEM ($n \geq 3$) is from HCV-Luc infection assay; CC_{50} ± SEM ($n \geq 3$) is from ATPlite cytotoxicity assay; Selectivity index = CC_{50}/EC_{50}.

[b] All compounds were tested at 10 μM, except that compounds **(S)-1**, **Rac-23** and **Rac-29** were tested at 3.2, 3.2 and 1 μM respectively to avoid potential cytotoxicity.

[c] Assay description: H1HR assay addresses the H_1-histamine receptor (H1HR) inhibitory activity. The numeric value corresponds to the percentage of activation induced by Histamine (250 nM) in the presence of 10 nM of compound; HCVsc assay applies single-round infectious HCV to detect inhibition of early stage prior to assembly in the virus replication cycle; HCVpp assay uses HCV pseudoparticle to determine HCVpp entry inhibition, while murine leukemia virus pseudoparticle (MLVpp) and vesicular stomatitis virus G pseudoparticle (VSV-Gpp) were tested as control to address viral specificity; In the HCV subgenomic replicon assay, genotype 2a HCV replicon cell line was used to evaluated the inhibitory effect of HCV RNA replication.

FIGURES

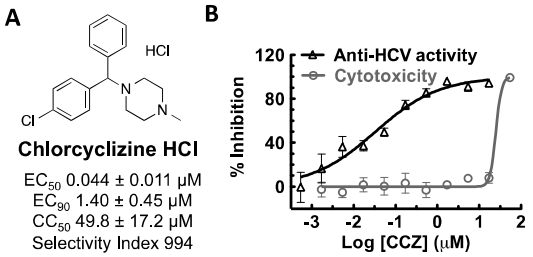

Figure 1. Chlorcylizine HCl identified from qHTS. (A) Chemical structure of chlorcylizine HCl (CCZ, **Rac-2**). (B) Anti-HCV activity and selectivity of chlorcyclizine HCl.

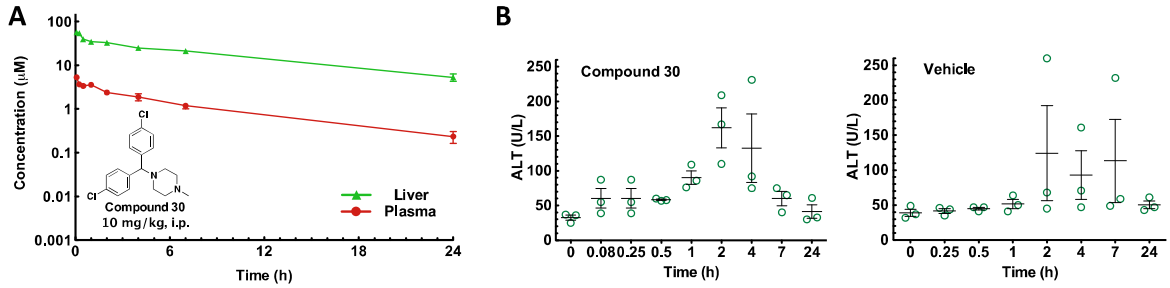

C

PK parameters	Compound **30**, 10 mg/kg, i.p., 24 h			Compound **(S)-2**, 50 mg/kg, i.p., 24 h			Compound **(S)-1**, 10 mg/kg, i.p., 24 h		
	Plasma	Liver	Liver/Plasma	Plasma	Liver	Liver/Plasma	Plasma	Liver	Liver/Plasma
AUC_{last} (h•μM)	27.5	429	16	48.9	1310	27	22.4	1259	56
AUC_{INF} (h•μM)	29.8	495	17	48.9	1310	27	22.9	1301	57
$T_{1/2}$ (h)	6.7	8.5	–	2.0	2.0	–	4.5	4.7	–
T_{max} (h)	0.083	0.083	–	0.25	0.083	–	1.00	0.083	–
C_{max} (μM)	5.28	57.0	11	16.1	436	27	3.71	216	58

Figure 2. In vivo pharmacokinetics profile of the lead compounds. (A) Plasma and liver samples were collected at indicated time points after a single i.p. dosing of compound **30** at 10 mg/kg in mouse model. Concentrations were measured using UPLC-MS/MS methods. (B) Alanine transaminase level of mouse serum samples collected from the pharmacokinetic study. Result of each mouse was shown with scatter plots and error bars show means ± SEM. (C) Pharmacokinetics parameters of compound **30** in comparison with previously reported results of compounds **(S)-2** and **(S)-1**.

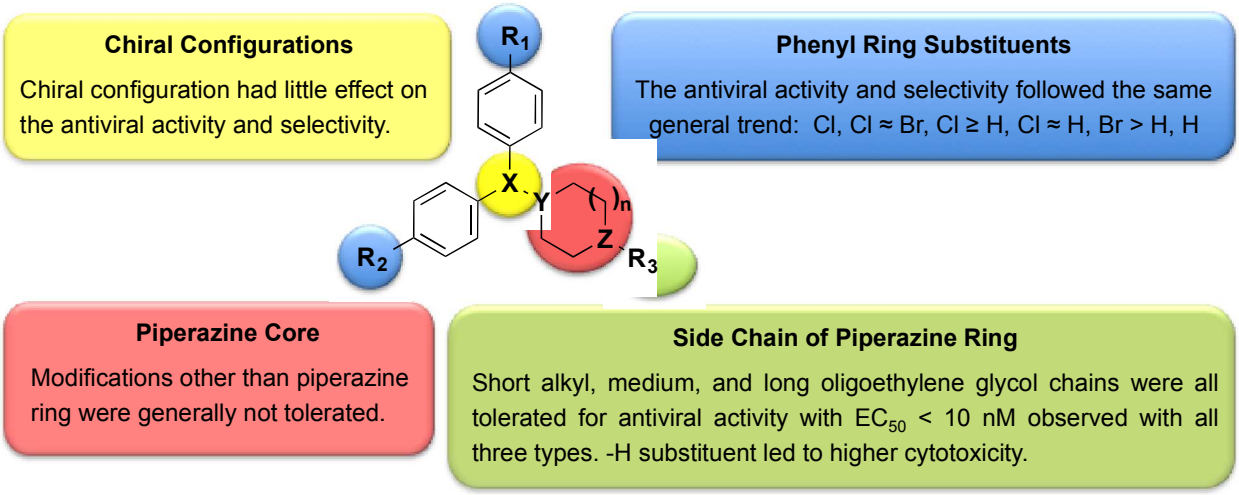

Figure 3. SAR summary.

SCHEMES

Scheme 1. General synthetic route for analogues shown in Table 1 (A) with alkyl substituents and (B) with oligoethylene glycol side chain

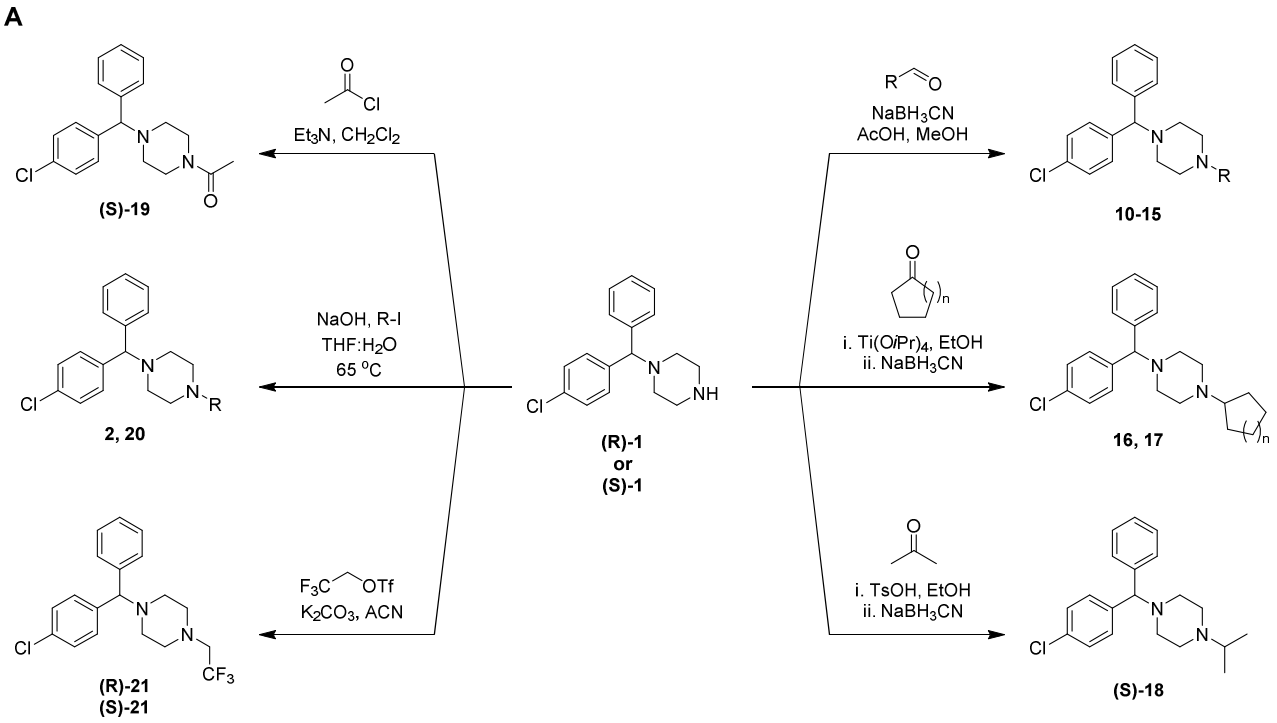

B

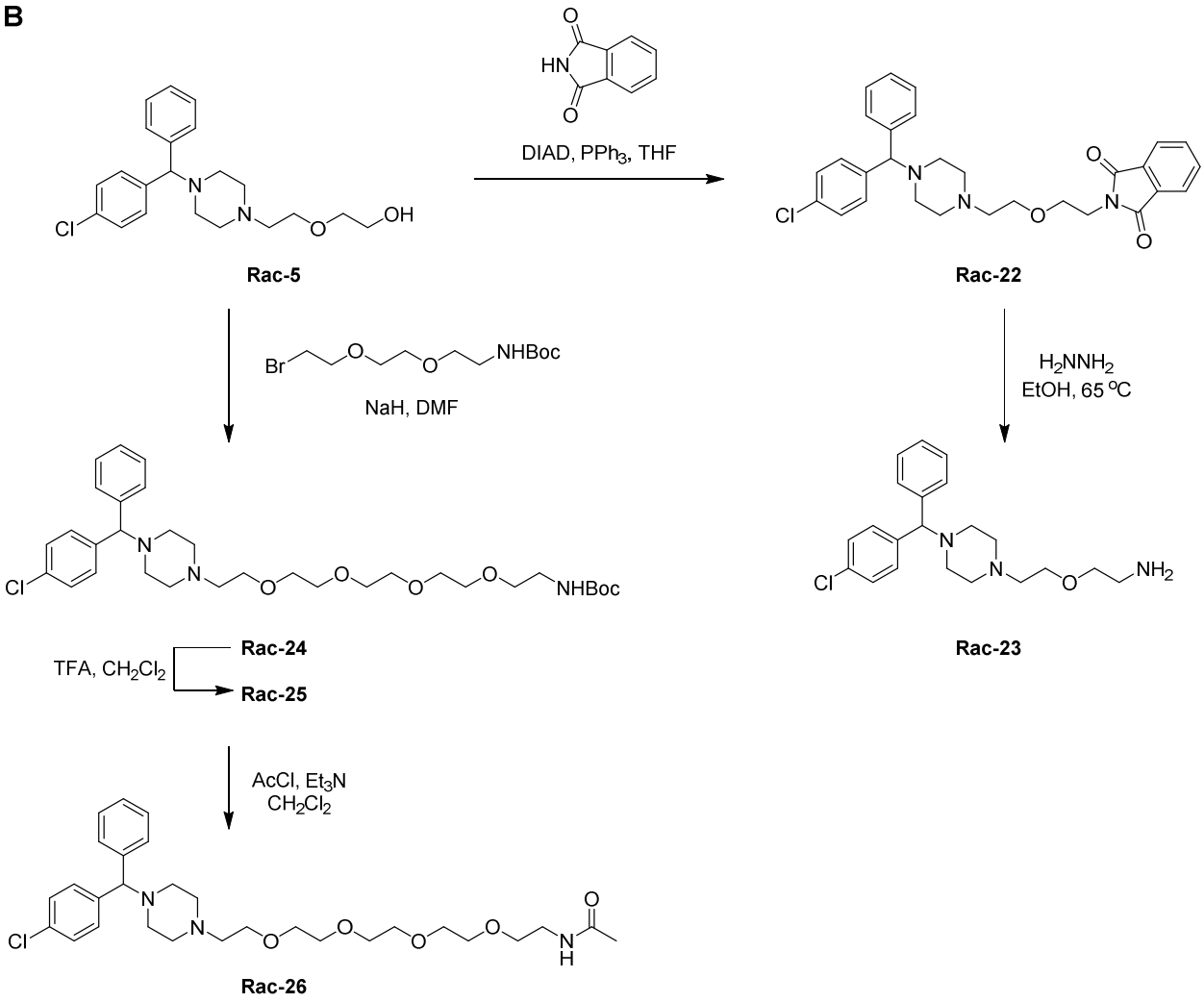
DIAD, PPh3, THF
Rac-5
Rac-22
NaH, DMF
H2NNH2
EtOH, 65 °C
Rac-24
Rac-23
TFA, CH2Cl2
Rac-25
AcCl, Et3N
CH2Cl2
Rac-26

Scheme 2. General synthetic route for analogues shown in Table 2 (A) with two chlorine substituents and (B) with bromide substituents

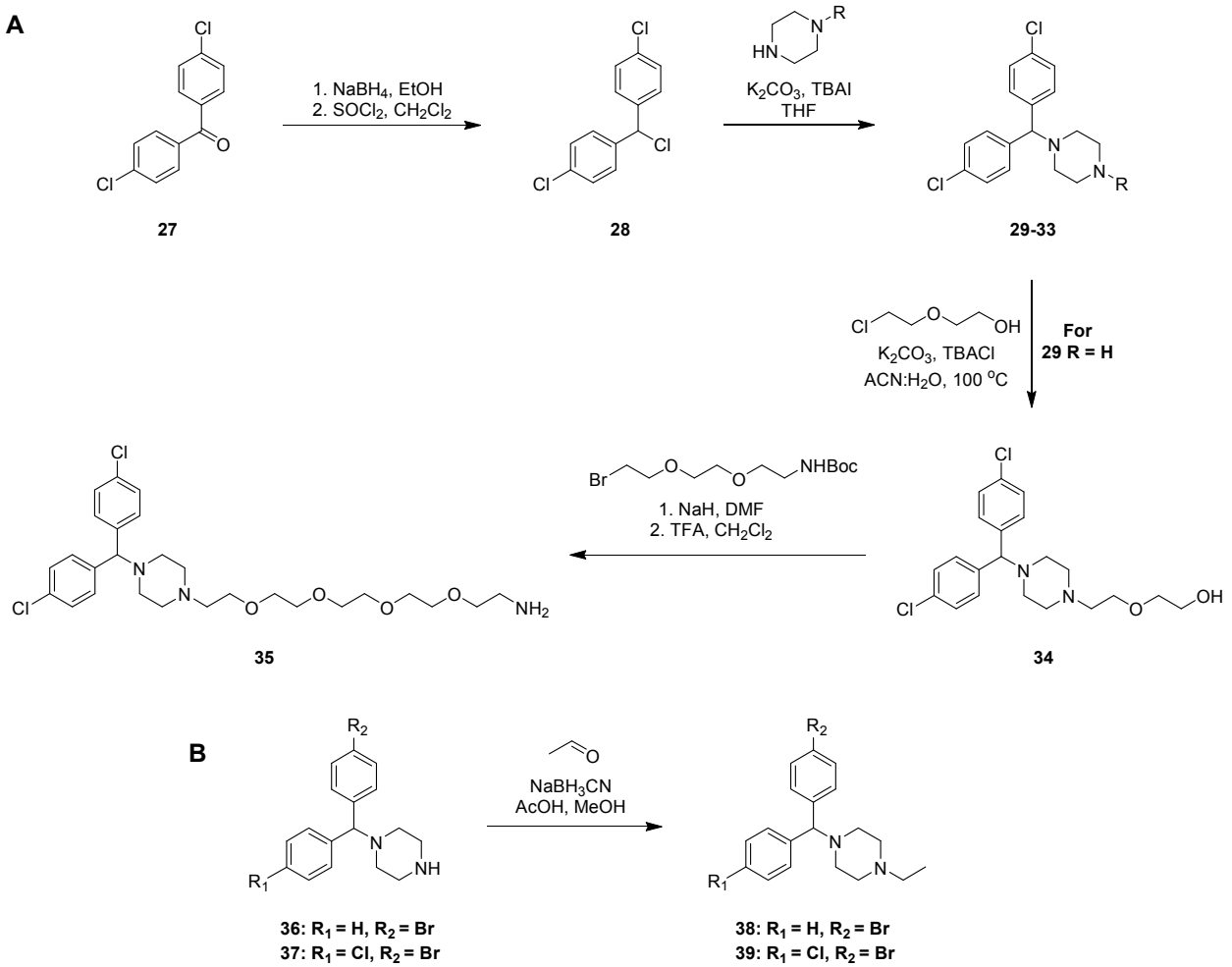

Scheme 3. General synthetic route for analogues shown in Table 3 (A) compound **44** and **45**, (B) compound **48.**

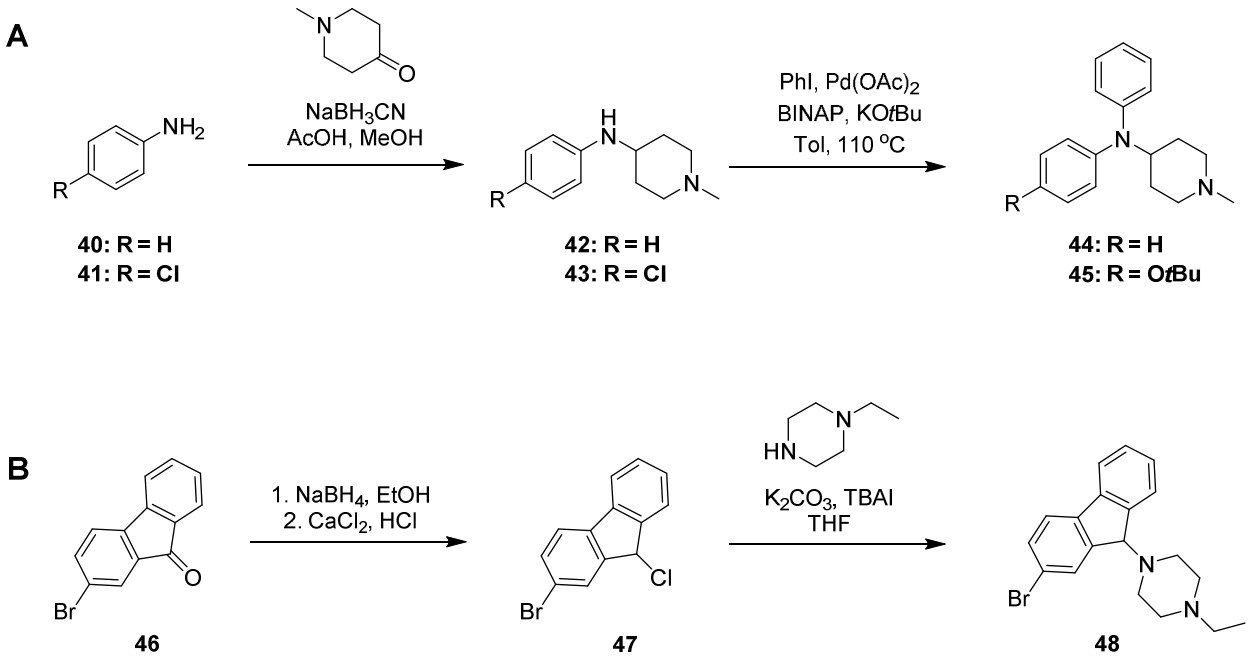

Table of Contents Graphic